Structure of Cd-Ga-Melts

Part 1: X-Ray High-Angle Scattering and Ultrasonic-Measurements

Gerhard Hermann, Richard Bek, and Siegfried Steeb

Max-Planck-Institut für Metallforschung, Institut für Werkstoffwissenschaften, Stuttgart

Z. Naturforsch. **35a**, 930–937 (1980); received June 30, 1980

By means of X-ray scattering and ultrasonic experiments, the structure of different melts of the Cd-Ga system was investigated. The structure factors $S(q)$ obtained for the pure elements agree well with those reported by other authors. The concentration dependence of the structure factors shows no special features. From the structure factors, the total pair-distribution functions were calculated by a Fourier transformation. The nearest-neighbour distances, obtained from the total pair-distribution functions, amount to 3.04 Å for pure Cd and 2.83 Å for pure Ga and are nearly constant for all alloys. The concentration dependence of the experimental nearest-neighbour distances and coordination numbers was determined and is compared with statistical distribution and macroscopic segregation models. These comparisons tend to indicate a preference for like-atom neighbours. From the long-wavelength limit $S(0)$ of the structure factors of Cd and Ga, the isothermal compressibilities were calculated. These show a satisfactory agreement with those calculated from adiabatic sound velocity data. The anomalous ultrasonic absorption of a single melt with nearly critical concentration indicates the existence of concentration fluctuations. This result is in agreement with those obtained by X-ray smallangle scattering experiments which are described in Part 2 of this work [1].

1. Introduction

In the molten state, the Cd-Ga system exhibits a closed miscibility gap (see Fig. 1) and the surrounding single phase region shows a strong short-range ordering. The liquidus line is rather flat. Therefore isothermal scattering experiments may be performed just above the liquidus temperature over almost the entire range of concentration. Thus, the influence of the temperature can be excluded during the discussion of the concentration dependence in the experimental results. Also, the critical temperature, T_c, which is relatively low compared to other metallic binaries, allows one to investigate a large region of the reduced temperature, $(T-T_c)/T_c$.

In the present paper high-angle X-ray scattering and ultrasonic velocity and absorption measurements have been used. Part 2 describes the small-angle X-ray scattering experiments [1].

2. X-Ray High-Angle Scattering

2.1. Theoretical fundamentals

X-ray scattering experiments were performed on different Cd-Ga melts with Mo-Kα-radiation. The intensity curves were corrected for polarization, absorption [2, 3], and incoherent scattering. The normalization procedure was done according to [4].

Reprint requests to Prof. Dr. S. Steeb, Max-Planck-Institut für Metallforschung, Seestraße 92, D-7000 Stuttgart 1.

The atomic form factors were taken from [5] and corrected for anomalous dispersion according to [6]. Thus the coherent scattered intensity, $I_{\mathrm{coh}}(q)$, was obtained, where the momentum transfer $q = 4\pi \frac{\sin\Theta}{\lambda}$, 2Θ = scattering angle, and λ = wavelength.

From $I_{\mathrm{coh}}(q)$ the total structure factor $S(q)$ was calculated using the following:

$$S(q) = \frac{I_{\mathrm{coh}}(q)}{\langle f^2 \rangle} = 1 + \varrho_0 \int_0^\infty [g(r) - 1] \frac{\sin q r}{q r} 4\pi r^2 \, \mathrm{d}r \tag{1}$$

where

f = scattering amplitude,
ϱ_0 = mean atomic number density,
$g(r) = \varrho(r)/\varrho_0$ = total pair-distribution function,
$\varrho(r)$ = total local atomic number density,
r = coordinate in real space.

The total pair-distribution function follows explicitly from a Fourier transformation of the structure factor and yields the total atomic distances and the total coordination numbers. To obtain the physically relevant partial quantities from the total quantities mentioned above, the total strucure factor has to be divided into the partial structure factors according to, for example, [7].

0340-4811 / 80 / 0900-0930 $ 01.00/0. — Please order a reprint rather than making your own copy.

In the long-wavelength limit, $q = 0$, the following equation holds for pure liquids:

$$S(0) = \varrho_0 k_B T \varkappa_T \tag{2}$$

where k_B = Boltzmann constant, T = temperature [K], $\varkappa_T$ = isothermal compressibility.
The isothermal compressibility, $\varkappa_T$, can be calculated from the adiabatic sound velocity by the relation

$$\varkappa_T = \frac{1}{D_M u_{ad}^2} + \frac{\alpha^2 T}{c_p D_M} \tag{3}$$

where u_{ad} = adiabatic sound velocity, D_M = macroscopic density, α = coefficient of volume expansion, c_p = specific heat at constant pressure.

2.2. *Experimental procedure*

2.2.1. The Cd-Ga system

Figure 1 shows the phase diagram of the Cd-Ga system established by means of a differential thermal analysis [8]. It exhibits a flat, closed miscibility gap in the liquid state over a concentration range of about 50 at%. The critical temperature of 295 °C is only 13° above the monotectic temperature of 282 °C.

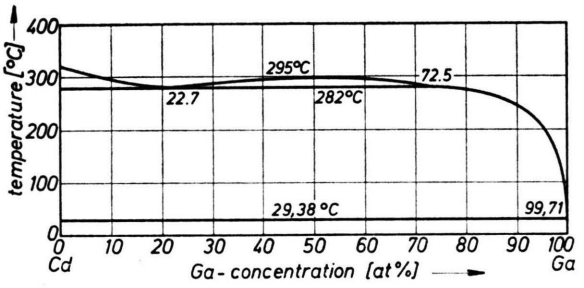

Fig. 1. Cd-Ga-System: phase diagram.

In the solid state Cd and Ga are nearly insoluble. In Ref. [9] the isotherms of the thermodynamic activities of Cd and Ga in Cd-Ga melts were determined by a vapor pressure comparison method in a temperature region from 130 °C up to 300 °C above T_c. The activity isotherms show a strong positive deviation from Raoult's law, indicating a segregation tendency even in this temperature region. The integral and partial enthalpies, energies, and entropies of mixing calculated in Ref. [10] from these data are in good agreement with the values reported in [11]. The temperature dependency of the structure sensitive properties, such as viscosity and thermal as well as electrical conductivity, also confirms the segregation tendency in Cd-Ga melts [12, 13, 14]. The density and compressibility data required for the quantitative evaluation of the scattering experiments were obtained from Refs. [15, 16]. The density isotherm at 350 °C yields a small relative excess volume of less than 3% compared to ideal behaviour.

2.2.2. Scattering apparatus

In part 1 and 2 of the present work, the atomic structure of Cd-Ga melts was determined. Because of the evidence for a segregation tendency in these melts, a small-angle scattering effect is to be expected as well as the usual high-angle scattering. Therefore the application of a scattering apparatus covering the entire angular range ($0.05\,\text{Å}^{-1} \leqq q \leqq 7.5\,\text{Å}^{-1}$) was required. Figure 2 shows schematically the main features of this apparatus [17].

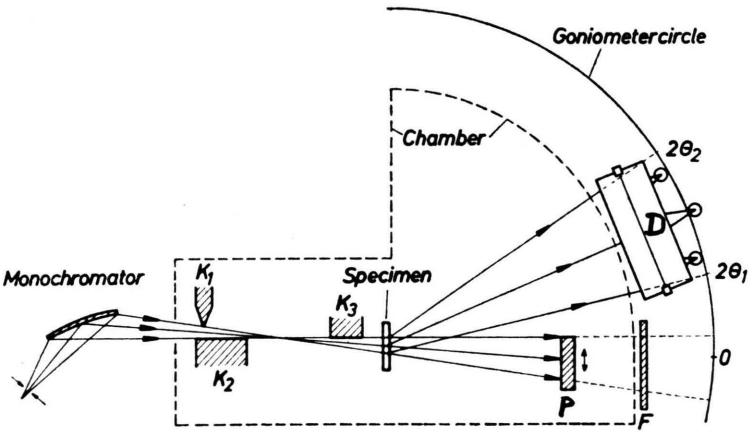

Fig. 2. Schematic diagram of scattering apparatus.

The Mo-Kα radiation is obtained from a 12 kW rotating-anode assembly * with a graphite monochromator. The double-walled chamber is water-cooled and can be evacuated. It contains the water-cooled Kratky-type collimation system (K_1, K_2, K_3), a thermostat with the specimen and the primary beam stop P.

The collimation system and the beam stop can be adjusted, and the sample can be lifted out of the X-ray-path from outside the evacuated chamber. The absorption foils, F, are used in order not to destroy the detector, D, during the determination of the intensity and the profile of the main beam. The position-sensitive detector, D **, has an effective length of 50 mm corresponding to an angular range $\Delta 2\,\Theta = 8°$ for the beam geometry used. Thus, the entire small-angle region up to $q = 1.2\,\text{Å}^{-1}$ can be covered during a single measurement without moving the detector. The high-angle scattering data are obtained with several detector positions and overlapping measurement ranges. The sealed position-sensitive X-ray detector consists essentially of a high-impedance counting wire and a xenon-methane-mixture used as counting gas. The position resolution of the detector was determined to be about 200 µm, corresponding to $\Delta(2\,\Theta) = 0.04°$, the energy resolution amounts to about 20%. The advantages of the position-sensitive detector, compared to the usual scintillation counters, are a reduced counting time and the elimination of the influence of temporary variations, caused, for example, by variations of the primary intensity, on the scattering curve.

With the position-sensitive detector care must be taken to compensate for non-linearities of the probability of detection along the counting wire, caused, for example by aging. The non-linearities may be detected and corrected by use of an isotropic radiating fluorescence or radioactive specimen.

2.2.3. Sample preparation and container

The optimum thickness for the Cd-Ga melts amounts to between 30 µm and 40 µm using Mo-Kα-radiation. According to the sample composition pure Cd (99.999%, Cerac, Milwaukee) and Ga (99.99%, Alusuisse, Neuhausen) were melted and mixed under inert gas atmosphere in an inducation furnace. The molten alloy was cast into a copper mold cooled by liquid nitrogen to avoid macroscopic segregation of the samples during solidification. The samples thus obtained were milled off to obtain optimum thickness by means of a micro-mill * with a specially designed supporting system. The latter held the samples by means of a vacuum. The final samples were plane parallel with deviations smaller than 1 µm. The composition of the sample sheets was checked by means of X-ray-fluorescence analysis.

The sample sheets ($20 \times 6 \times 0{,}035\,\text{mm}^3$) were then put into the opening of a tantalum frame ($30 \times 40\,\text{mm}^2$) with exactly the same thickness as the sample. The sample sheets with the frame were then masked from both sides by thin, plane parallel mica sheets used as window material, and the whole "sandwich" was screwed in between polished copper frames of 1.5 mm thickness. Sapphire disks were also used as window material.

2.2.4. Performance of experiments

The high-angle scattering experiments were performed with the pure elements Cd and Ga and seven alloys of the Cd-Ga system. The alloys and pure Ga were studied at 296 °C, i. e., about 1° above the critical temperature. Pure Cd was studied at 325 °C. The pure elements and some alloys were additionally investigated at other temperatures to determine an eventual temperature dependence of quantities such as main peak position and height of the structure factor or coordination number. The temperature measurement and control was carried out by a NiCr-Ni-thermocouple and a high precision PID-controller with extreme long-period stability. An ice-water mixture was used as the reference temperature. The temperature gradient in the sample was determined to be less than ± 0.15 °C at 300 °C. The absolute temperature calibration was done by using the melting and solidification temperatures of different metals.

Before starting the measurement, the molten Cd-Ga specimens were annealed several hours at a temperature of 50 °C above the critical temperature though no significant changes of the scattered intensity were detected during this annealing procedure. Thus homogeneous mixing was assured. Thermal equilibrium was achieved during a few minutes.

* Rigaku-Denki, Tokyo.
** CGR, Paris.

* Jung, Nußloch.

Also, no thermal hysteresis effects could be observed after several temperature cycles. The high-angle as well as the small-angle scattering experiments showed high reproducibility.

2.3. Results and discussion

2.3.1. Structure factors

The Figs. 3 a and 3 b show the total structure factors from the pure components Cd and Ga and from seven alloys.

2.3.1.1. Molten Cd and Ga

Since Cd exhibits an extremely large absorption cross section for thermal neutrons, no neutron scattering results have been reported until now. X-ray data are given in [18, 19, 20]. The position of the three main maxima in $S(q)$ as well as the height of the first maximum $S(q_1)$, as reported in [19, 20], are in good agreement with the present values. Good agreement with the literature values is also found for the structure factors measured at 360 °C and 440 °C. The shape of the structure factor curve of Cd is substantially identical to the shape expected for monatomic metallic melts and shows only a slight temperature dependence.

Molten Ga has been investigated by means of X-ray and neutron diffraction within the temperature range from -110 °C up to 1000 °C [19, 21, 22, 23]. In Fig. 4 the structure factors obtained during the present work at 30 °C and 296 °C are compared. At higher temperatures the pronounced shoulder at $q \sim 3.1$ Å^{-1} apparently tends to vanish. The position of the first maximum remains nearly unchanged whereas its height is drastically reduced from 2.50 to 1.95 at 296 °C and finally reaches 1.80 at 600 °C. The shoulder mentioned above can be explained by assuming a special arrangement of Ga-atoms in addition to the "free" Ga-atoms which are considered to behave like hard spheres. The structure of this special arrangement is discussed in different ways [22, 23, 24] and is, at present, not yet fully understood. In any case, at temperatures above 300 °C the Ga-melt consists merely of "free" atoms.

The structure factors of the pure liquid elements Cd and Ga are low for small momentum transfers, i. e. small q, and can easily be extrapolated to $q = 0$. From the values $S(0)$ thus obtained, the isothermal

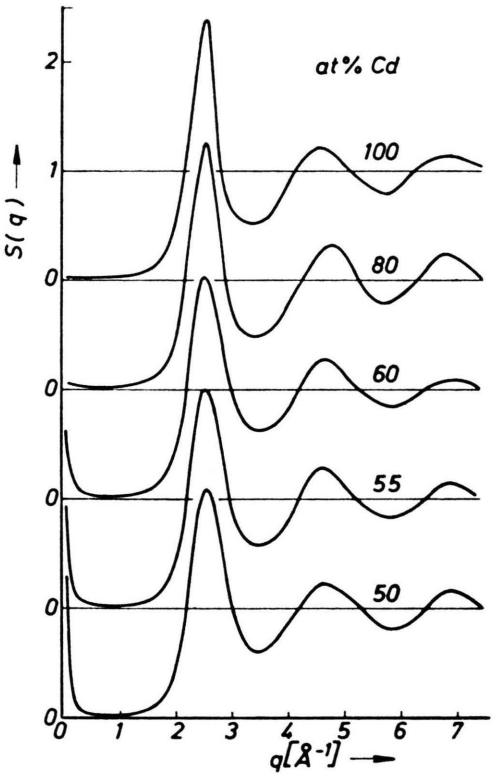

Fig. 3a. Cd-Ga-system: structure factors $S(q)$. $T = 296$ °C. Only for 100 at % Cd: $T = 325$ °C.

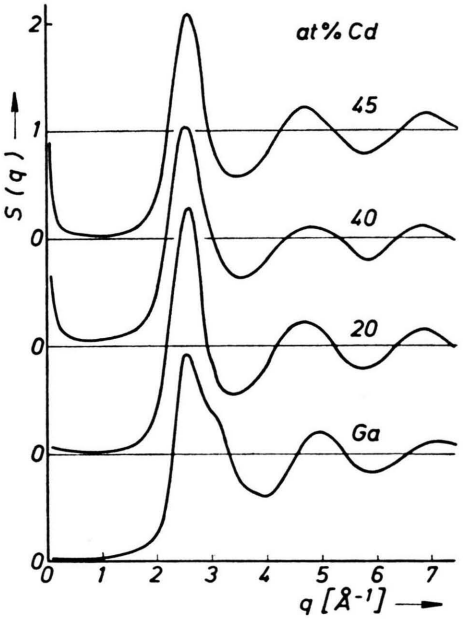

Fig. 3b. Cd-Ga-system: structure factors $S(q)$. $T = 296$ °C

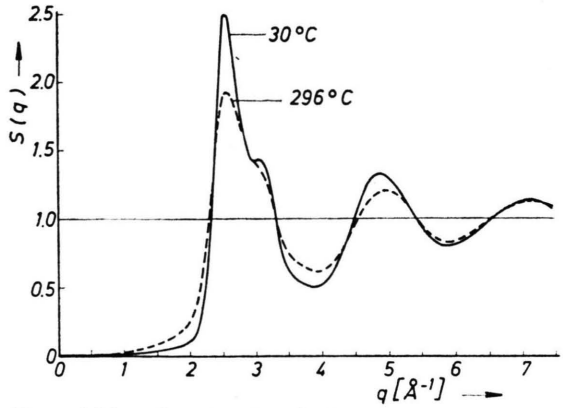

Fig. 4. Molten Ga: structure factor.

compressibilities, $\varkappa_T$, were calculated according to Equation (2). The data are compiled in Table 1.

Table 1. Molten Cd and Ga: structure factors $S(0)$ and isothermal compressibilities.

Element	Temperature T (°C)	$S(0)$	$\varkappa_T \cdot 10^{12}$ from $S(0)$ $\left[\frac{\text{cm sec}^2}{\text{g}}\right]$
Cd	325	0.012	3.39
Ga	30	0.0065	2.96
Ga	296	0.012	3.24

These compressibility values are between 5% and 17% larger than those values calculated from Eq. (3) using adiabatic sound velocity data from [25]. Since the intensity of the small-angle scattering by the liquid elements shows no rise as $q \to 0$, the statistical error of the structure factors amounts to about 10%. The reason for this error is that in the cases of non-increasing intensity as $q \to 0$, the scattering due to the container has the same order of magnitude as the scattering due to the melt. Thus, the variation of the compressibility data is not unreasonable. This is not true for the alloys treated in [1], for which the scattering due to the melts exceeds the background scattering by far.

2.3.1.2. Molten alloys

The position of the first maximum in Figs. 3 a and 3 b remains virtually unchanged at $q_1 \sim 2.55\,\text{Å}^{-1}$ and is shifted only slightly to higher q-values at higher Cd-concentrations. Since the positions of the first maximum of the structure factors of molten Ga and Cd are nearly the same, the structure factors of the molten alloys show no indication for segregation. Segregation phenomena, such as a broadening or splitting of the alloy structure factor curve, cannot be observed. The height of the first maximum decreases rapidly starting from pure Cd ($S(q_1) = 2.5$) and then remains constant in the entire concentration range. For mean concentrations the shape of the first maximum is nearly symmetric. The shoulder still visible for Ga at 296 °C has vanished at concentrations of more than 20 at % Cd. The q-values of the second and third maximum increase slightly with rising Ga-content. The most interesting feature in Figs. 3 a and 3 b, namely the rise for $q \to 0$ especially for mean concentrations, will be discussed in [1].

2.3.2. Pair-distribution functions

Figure 5 shows the total pair-distribution functions $g_t(r)$ obtained by Fourier transformation from the

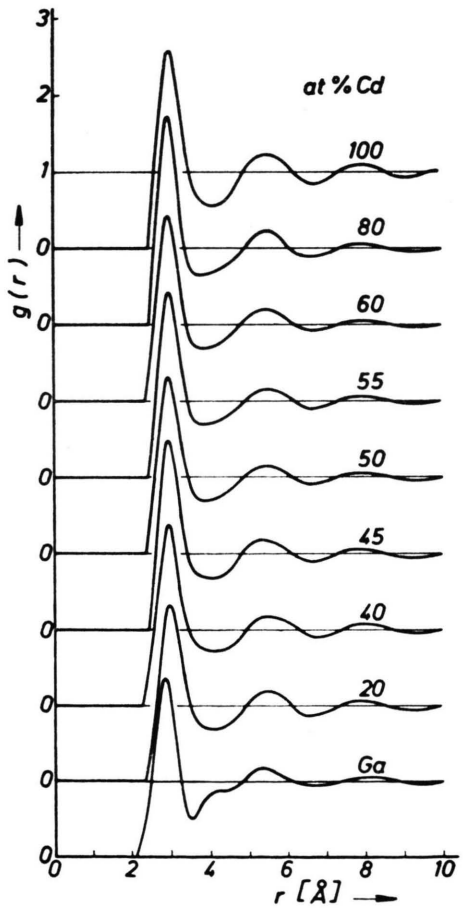

Fig. 5. Cd-Ga-system: pair-distribution function $g_t(r)$. $T = 296$ °C. Only for 100 at % Cd: $T = 325$ °C.

total structure factors. The physically non-relevant oscillations below $r = 2$ Å induced by the finite integration length are already eliminated and replaced by $g_t(r) \equiv 0$.

From Fig. 5 it is extracted that the distance between nearest-neighbours amounts to between $r^I = 3.04$ Å for pure Cd and $r^I = 2.83$ Å for pure Ga. This nearest-neighbour distance is nearly constant for all alloys and varies only as $2.95\,\text{Å} \leqq r_t^I \leqq 3.0\,\text{Å}$. The accuracy for the r_t^I-values for different integration lengths amounts to ± 0.02 Å. Pure Ga at 296 °C exhibits a small subsidiary maximum at $r \sim 4$ Å which also appears in the pair-distribution function of Ga at 30 °C. In Ref. [26] a similar maximum was found for liquid antimony to which covalent bindings are attributed. The subsidiary maximum in the pair-distribution function of liquid Ga and the shoulder in the structure factor both vanish upon alloying with more than 20 at% in the melt.

The experimental coordination numbers, N_t^I, were calculated from the area under the first maximum of the atomic distribution curve, $A_t(r) = 4\pi r^2 \varrho_0 g_t(r)$. In the case of the alloys, however, the N_t^I are weighted by the scattering power of the elements. Nevertheless, results about the structural features of the melts of a system can be deduced from the concentration dependence of r_t^I and N_t^I. Doing this, the cases of compound formation and segregation have to be distinguished as follows.

If compound formation in the melt occurs, a reduction of the true radii and coordination numbers is expected. Macroscopically one often observes a large decrease of the molar volume. This reduction of the true, unweighted quantities also influences the experimentally measured, weighted quantities, such as r_t^I and N_t^I. In the case of segregation, for metallic melts with nearly the same coordination number of the pure components, the variation with concentration of the true radii and coordination numbers corresponds substantially to that expected for random distribution of the atoms. Nevertheless, some evidence about the structural features of those melts can be obtained by comparing the experimental r_t^I and N_t^I with those values obtained from the models of random or statistical distribution and macroscopic segregation, respectively. These quantities r_{st}^I and N_{st}^I or r_{segr}^I and N_{segr}^I are also weighted by the scattering powers of the elements. Thus, the following equations are obtained [27]:

$$\Delta r^I = r_{segr}^I - r_{st}^I = \frac{c_A c_B f_A f_B (r_A^I - r_B^I)(f_B N_B^I - f_A N_A^I)}{\langle f \rangle (c_A f_A^2 N_A^I + c_B f_B^2 N_B^I)}, \tag{4}$$

$$\Delta N^I = N_{segr}^I - N_{st}^I = \frac{c_A c_B (f_B - f_A)[N_B^I (f_B + \langle f \rangle) - N_A^I (f_A + \langle f \rangle)]}{\langle f \rangle^2}. \tag{5}$$

Obviously, Δr^I is small if $r_A^I \sim r_B^I$ and if the element with the smaller coordination number exhibits the larger scattering power. This is true for Cd-Ga melts. ΔN^I is small if $f_A^I \sim f_B^I$.

Figure 6 shows the dependence of the experimental values r_t^I and N_t^I with the concentration and a comparison with those values calculated for the models of statistical distribution and macroscopic segregation, respectively. The experimental values lie essentially between the curves obtained for the two models mentioned above. This indicates a preference for like nearest-neighbours or the existence of concentration fluctuations, respectively. However, the small differences between the values calculated for the two model systems do not allow for unambigous conclusions. The reason is that the values of r^I and N^I for pure Cd and Ga only differ by about 7%.

Moreover, the Fourier transform of a high-angle scattering curve, $g_t(r)$, from a binary melt describes the spatial environment of a fictive "mean" atom with regards to distances and number of nearest-neighbours. In the case of Cd-Ga melts, those quantities are only slightly influenced by the chemical short-range order such as preferred like neighbours or the statistical random distribution of the atoms. Direct indication for the concentration fluctuations existing in Cd-Ga melts can only be obtained by the small-angle scattering experiments described in Ref. [1], or by the ultrasonic velocity and absorption measurements described in the following chapter.

3. Ultrasonic Measurements

The ultrasonic velocity and absorption studies were performed for only one melt of the Cd-Ga

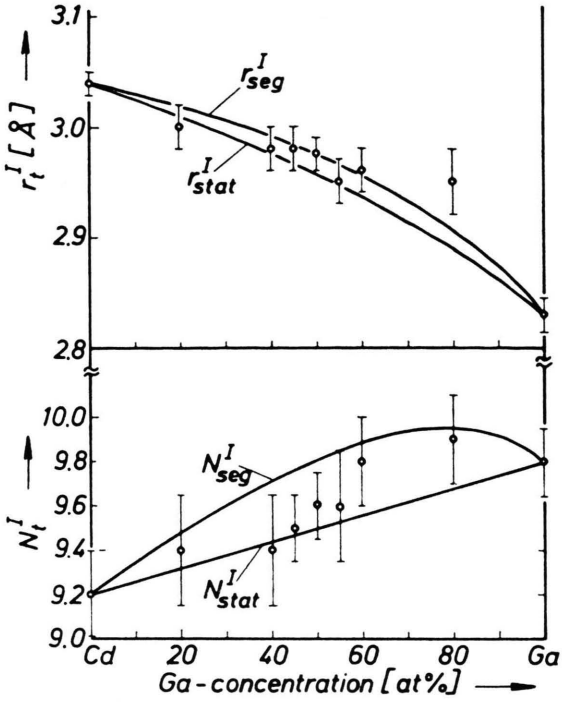

Fig. 6. Cd-Ga-system: radii r_t^I and coordination numbers N_t^I of the first coordination sphere.

system. An almost critical composition melt, i.e. 55 at% Ga, was used in a procedure described in [28]. The ultrasonic velocity was measured to check the values given in [16]. These data were used previously to calcule the isothermal compressibility which is required for the analysis of the small-angle scattering experiments described in [1]. With the same experimental equipment as used in [28], a frequency dependent ultrasonic absorption study was made. According to the Fixman-theory [29], an anomalous behaviour of the absorption in the critical region could be expected.

Classical ultrasonic absorption in liquids is due to energy losses by heat conduction and viscosity. In liquid metals, losses by heat conduction exceed by far the other contributions. Classical absorption is proportional to the square of the frequency of the sound wave. An anomalous behaviour in the absorption in the critical region can be understood in the following way according to [29]: the adiabatic sound wave induces changes in the pressure accompanied by changes in the temperature. In the critical region small changes in temperature are associated with large structural changes.

The strong temperature dependence of the correlation length of the concentration fluctuations, described in [1], is an illustration of this. According to Fixman, the anomalous absorption is mainly caused by the delayed response of the liquid system to the temperature fluctuations induced by the sound wave. This assumption leads to the introduction of a frequency dependent heat capacity, which, in turn, is related to the frequency dependent anomalous ultrasonic absorption. Accordingly, the following proportionality should be valid:

$$\alpha/f^2 \sim f^{-5/4} \tag{6}$$

where α = absorption coefficient, f = ultrasonic frequency. Thus, a graph of α/f^2 versus temperature for different frequencies indicates directly the anomalous behaviour of absorption by a frequency dependent rise of α/f^2 in the critical region. This rise is stronger for lower frequencies.

Experiments ([28]) were carried out by means of a pulse echo technique in the frequency range between 30 MHz and 90 MHz. Direct measurements were made of the travel time and amplitude of the reflected signal. A homogeneous mixture of the melt was obtained only after heating the sample 80 °C above the critical temperature for about 16 hours. During this time, the melt was rapidly stirred. For the X-ray scattering experiments it was determined that thermal equilibrium within the melts was achieved within minutes. The different behaviour can be explained by noting that the samples for the X-ray experiments had already been "homogenized" by rapid quenching from a homogeneous liquid phase. Also, the volume of the sample for the ultrasonic experiments was about 10^4 times larger than that of the samples for the X-ray experiments.

Figure 7 shows the temperature dependence of the ultrasonic velocity and absorption measurements in a Cd-Ga melt of 55 at% Ga for different frequencies between 30 MHz and 90 MHz.

The ultrasonic velocity and thus the adiabatic compressibility exhibit no critical effects in the region of the homogeneous melt above 295 °C. At about 295 °C, the phase separation line appears as a discontinuity in the ultrasonic velocity. The same observation was made for the Bi-Ga system in [30].

In the temperature range between 350 °C and 400 °C, the temperature coefficient of the ultrasonic velocity changes from about 21 to 36 cm/sec °C. According to Refs. [17, 25] such a behaviour indi-

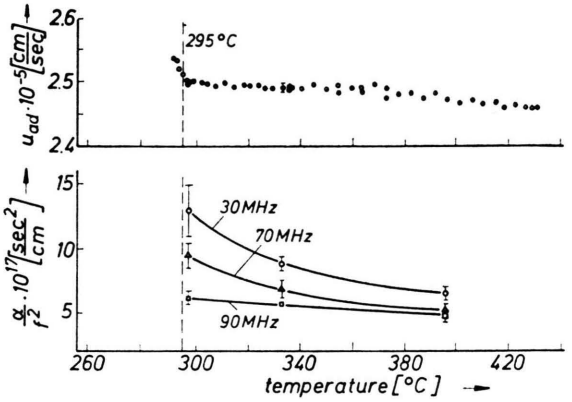

Fig. 7. Cd-Ga-system (55 at% Ga): ultrasonic-velocity and absorption.

cates structural changes in the melt which, in the present case, may be related to the decrease of the concentration fluctuations in the melt. This outcome is in accordance with the results of the X-ray small-angle scattering experiments presented in [1]. Also, the ultrasonic velocity exhibits no dispersion.

If the ratio α/f^2 is plotted as a function of temperature T, the ultrasonic absorption distinctly increases upon approaching the critical temperature in the homogeneous melt. This rise is more distinct for lower frequencies in qualitative agreement with the theoretical predictions. This anomalous, critical absorption which cannot be explained by the classical predictions confirms the existence of concentration fluctuations.

A quantitative analysis of the absorption measurements requires experimental results over the entire concentration range. Thus, comparisons with the results of the critical X-ray scattering measurements could be made. But, to date, no such comparison has been reported in the literature concerning metallic systems.

In the present work, the measurements of the ultrasonic velocity confirmed the normal behaviour of the adiabatic compressibility in the homogeneous phase near the critical point. However, the anomalous ultrasonic absorption gave strong indications for the existence of concentration fluctuations in the homogeneous melts of the Cd-Ga system.

Acknowledgements

Thanks are due to DFG for financial support of part of this investigation.

[1] G. Hermann, G. Rainer-Harbach, and S. Steeb, Z. Naturforsch. **35a**, 938 (1980), Part 2.
[2] H. H. Paalman, C. J. Pings, J. Appl. Phys. **33**, 2635 (1962).
[3] G. Hermann, Dissertation, Universität Stuttgart 1980.
[4] J. Krogh-Moe, Acta Cryst. **9**, 951 (1956).
[5] D. T. Cromer and J. T. Waber, Acta Cryst. **18**, 104 (1965).
[6] D. T. Cromer, Acta Cryst. **18**, 17 (1965).
[7] N. W. Ashcroft and D. C. Langreth, Phys. Rev. **156**, 685 (1967).
[8] T. Heumann and B. Predel, Z. Metallkunde **49**, 90 (1958).
[9] B. Predel, Z. Metallkunde **49**, 226 (1958).
[10] R. Hultgren et al, "Selected Values of the Thermodynamic Properties of Binary Alloys", Amer. Soc. Met. 1973.
[11] G. R. B. Elliott, J. F. Lemons, and H. S. Swofford, J. Phys. Chem. **69**, 933 (1965).
[12] W. Menz and F. Sauerwald, Z. Phys. Chem. **232**, 134 (1966).
[13] A.-M. A. Magomedov, B. P. Pashayev, and M. A. Ismaylov, Russ. Met. **5**, 163 (1975).
[14] V. I. Kononenko, A. L. Sukhman, and V. G. Shevchenko, Russ. Met. **4**, 57 (1976).
[15] C. B. Chokonov, S. N. Zadumkin, B. B. Alcagirov, and B. S. Karamurzov, Izv. Sev. Kauk. **1**, 60 (1973).
[16] A.-M. A. Magomedov, M. A. Ismaylov, and B. P. Pashayev, Russ. Met. **1**, 159 (1975).
[17] J. Höhler, Dissertation, Universität Stuttgart 1975.
[18] C. Gamertsfelder, J. Chem. Phys. **9**, 450 (1941).
[19] C. N. J. Wagner, Inst. Phys. Conf. Ser. No. **30**, 110 (1977).
[20] A. V. Romanova, O. I. Sluchovskij, and M. Juris, Ukr. Fiz. Zh. **23**, 722 (1978).
[21] A. H. Narten, J. Chem. Phys. **56**, 1185 (1971).
[22] A. Bizid, A. Defrain, R. Bellissent, and G. Tourand, J. Physique **39**, 554 (1978).
[23] S. E. Rodriguez and C. J. Pings, J. Chem. Phys. **42**, 2435 (1965).
[24] N. H. March, M. Parrinello, and M. P. Tosi, Phys. Chem. Liq. **1**, 39 (1976).
[25] M. B. Gitis and I. G. Mikhailov, Sov. Phys. Acoust. **12**, 131 (1966).
[26] H. P. Lamparter, Dissertation, Universität 1976.
[27] J. P. Gabathuler, S. Steeb, and P. Lamparter, Z. Naturforsch. **34a**, 1305 (1979).
[28] R. Bek, Dissertation, Universität Stuttgart 1980.
[29] M. Fixman, J. Chem. Phys. **36**, 1961 (1962).
[30] M. P. Puls and J. S. Kirkaldy, J. Chem. Phys. **54**, 4468 (1971).